The selective estrogen receptor modulator clomiphene inhibits sterol biosynthesis in *Arabidopsis thaliana*

Qing Wang[1,2,*], Kjell De Vriese[1,2,*], Sandrien Desmet[3], Ren Wang[4], Markéta Luklová[4], Qianqian Liu[4], Jacob Pollier[3], Qing Lu[1,2], Sarah Schlag[5], Walter Vetter[5], Alain Goossens[1,2], Eugenia Russinova[1,2], Geert Goeminne[3], Danny Geelen[4], Tom Beeckman[1,2], Steffen Vanneste[1,2,4,‡]

1: Department of Plant Biotechnology and Bioinformatics, Ghent University, Technologiepark 71, B-9052 Ghent, Belgium

2: VIB Center for Plant Systems Biology, VIB, Technologiepark 71, B-9052 Ghent, Belgium

3: VIB Metabolomics Core Ghent, Technologiepark 71, B-9052 Ghent, Belgium

4: Department of Plants and Crops, Ghent University, Coupure Links 653, B-9000 Ghent, Belgium

5: University of Hohenheim, Institute of Food Chemistry (170b), Garbenstraße 28, D-70599 Stuttgart, Germany

*These authors contributed equally

‡ For correspondence

Highlight

We expand the pharmacology to manipulate plant sterol biosynthesis. Our findings reveal that bifonazole, clotrimazole, and econazole inhibit plant CYP51 and we identified clomiphene as a novel inhibitor of the plant-specific cyclopropyl-cycloisomerase.

Abstract

Sterols are produced via complex, multistep biosynthetic pathways involving similar enzymatic conversions in plants, animals and fungi, yielding a variety of sterol metabolites with slightly different chemical properties to exert diverse and specific functions. A tremendously diverse landscape of sterols, and sterol-derived compounds, can be found across the plant kingdom, determining a wide spectrum of functions. Resolving the underlying biosynthetic pathways is thus instrumental to understanding the function and use of these molecules. In only a few plants, sterol biosynthesis has been studied using mutants. In non-model species a pharmacological approach is required. However, this relies on only a few inhibitors. Here, we probed a collection of inhibitors of mammalian cholesterol biosynthesis to identify new inhibitors of plant sterol biosynthesis. We show that imidazole-type fungicides, bifonazole, clotrimazole and econazole inhibit the obtusifoliol 14α-demethylase CYP51 in plants. Moreover, we found that the selective estrogen receptor modulator, clomiphene, inhibits sterol biosynthesis in part by inhibiting the plant-specific cyclopropyl-cycloisomerase CPI1. These results demonstrate that rescreening of inhibitors animal sterol biosynthesis is an easy approach for identifying novel inhibitors of plant sterol biosynthesis. These molecules expand the toolkit for studying and manipulating sterol biosynthesis in the plant kingdom.

Keywords

Sterol biosynthesis; inhibitor; CYP51; cyclopropyl-cycloisomerase; hypocotyl; root; cell division; auxin; Arabidopsis

Abbreviations

Cytochrome P450 (CYP), CYCLOPROPYLSTEROL CYCLOISOMERASE1 (CPI1)

Introduction

Sterols mainly function as structural components of the plasma membrane where they regulate membrane permeability and fluidity, contribute to organizing the membrane, and modulate the activity of membrane-bound enzymes, such as plasma membrane H^+ ATPases (Cacas *et al.*, 2012; Gronnier *et al.*, 2017; Morales-Cedillo *et al.*, 2015; Schaller, 2003; Simon-Plas *et al.*, 2011). The importance of sterols in membrane functions, and their ubiquity among eukaryotes indicate that sterol biosynthesis is a key evolutionary innovation in eukaryotes (Chen *et al.*, 2007). Consistently, in plants, many cellular processes are sterol-dependent, such as clathrin-mediated endocytosis (Konopka *et al.*, 2008; Men *et al.*, 2008), cytokinesis (Boutte *et al.*, 2010; Nakamoto *et al.*, 2015), polarity (Men *et al.*, 2008; Stanislas *et al.*, 2015), and signaling (Simon-Plas *et al.*, 2011). Additionally, sterols are also important for processes at the endoplasmic reticulum, such as ethylene signaling (Zhao *et al.*, 2020), and are required for the formation of oleosin-coated lipid droplets (Yu *et al.*, 2021). At the macroscopic level misregulated phytosterol homeostasis results in various defects during embryonic and post-embryonic development (Clouse, 2000; Schaller, 2003), fertility (Azpiroz *et al.*, 1998; Catterou *et al.*, 2001), plant flowering (Schaller, 2003), growth (He *et al.*, 2000; Schaller, 2003), seed germination (Guo *et al.*, 1995), biotic- and abiotic stress responses (Han *et al.*, 2009; Kumar *et al.*, 2015; Pose *et al.*, 2009; Senthil-Kumar *et al.*, 2013), and the auxin-mediated regulation of cell polarity, gravitropism, endocytosis and auxin efflux (Men *et al.*, 2008; Pan *et al.*, 2009; Willemsen *et al.*, 2003; Yang *et al.*, 2013). Moreover, phytosterols are involved in many aspects of plant-microbe interactions (Der *et al.*, 2024), seed triacylglycerol content and seed morphology (Yu *et al.*, 2021).

Phytosterol biosynthesis is a complex, multistep process, involving the coordinated activity of distinct enzymes, converting cycloartenol into the major phytosterols β-sitosterol, stigmasterol and campesterol (De Vriese *et al.*, 2021) (Supplementary Fig. S1). Notably, an astonishing diversity of sterols and sterol-derived bioactive compounds can be found in the plant kingdom

through variations to the canonical phytosterol biosynthetic pathway (Darnet *et al.*, 2021; Moreau *et al.*, 2018). In example, a tomato STEROL SIDE CHAIN REDUCTASE2, that is not found in Arabidopsis, produces the precursor for cholesterol biosynthesis via largely the same enzymes as in for phytosterol biosynthesis (Sonawane *et al.*, 2016).

Many Arabidopsis mutants that are defective in processing of C4-methyl phytosterol intermediates such as CYCLOPROPYLSTEROL CYCLOISOMERASE1 (CPI1), CYP51G1, FACKEL/HYDRA (FK/HYD) and HYDRA1 (HYD1) STEROL METHYLTRANSFERASE1 (SMT1), and STEROL 4A-METHYL OXIDASE1 (SMO1) and SMO2 display a range of embryo and/or seedling development defects (Boutte and Grebe, 2009; Clouse, 2000; Diener *et al.*, 2000; Song *et al.*, 2019; Souter *et al.*, 2002; Zhang *et al.*, 2016). These strong phenotypes have been associated with misregulation of auxin, cytokinin and/or ethylene activities (Song *et al.*, 2019; Souter *et al.*, 2002; Wang *et al.*, 2021; Zhang *et al.*, 2016). Weak *smt2/frl1/cvp1* mutant alleles have modest developmental defects, such as serrated petals (Hase *et al.*, 2005), and discontinuous cotyledonary venation (Carland *et al.*, 2002). A double mutant with its closest ortholog (*smt3*) generates stronger phenotypes, including abnormal floral organs and root growth defects (Carland *et al.*, 2010). While single mutants *smo1-1*, *smo1-2* and the weakly expressed *smo1-3* do not show an obvious abnormal phenotype, *smo1-1smo1-2* double mutants displayed strong embryo developmental defects (Song *et al.*, 2019). These defects, resulting in aberrant embryonic and endosperm development, were stronger than in the *smo2-1smo2-2* double mutant (Zhang *et al.*, 2016). In contrast, mutants defective in enzymes acting post-C4-demethylation, such as *dwarf7/sterol1, dwarf5*, and *dwarf1/diminuto*, do not show such severe developmental defects. Instead, these mutants mainly display brassinosteroid-deficiency phenotypes, such as dwarfism and defects in fertility, cell elongation, flowering and senescence, which can be largely rescued by exogenous brassinosteroids (Choe et al., 1999a; Choe et al., 1999b; Choe et al., 2000; Klahre et al., 1998). Moreover, these mutants are also defective in the formation of oleosin-

coated lipid droplets, and seed development (Der *et al.*, 2024). The wide variety of phenotypes in mutants in the canonical sterol biosynthesis pathway indicates that these phenotypes might be dependent on the accumulation of specific sterol biosynthesis intermediates, rather than by the lack of the end-product sterol (Schrick *et al.*, 2004). In example, the phytosterol biosynthesis intermediate 4-carboxy-4-methyl-24-methylenecycloartanol was found to inhibit auxin transport (Mialoundama *et al.*, 2013). Similarly, the antifungal activity of azoles was recently shown to be due to the accumulation of the CYP51 ergosterol biosynthesis pathway substrate eburicol (Elsaman *et al.*, 2024).

While mutants are a great asset for the study of phytosterol and brassinosteroid biology in plants, they are not without drawbacks. For instance, the severe growth phenotypes that are typical for sterol and brassinosteroid biosynthesis mutants make it difficult to dissect what is direct or what is an indirect, pleiotropic effect due to the often strong developmental phenotypes in the mutants. Therefore, an interesting alternative to study phytosterol and BR biology in plants is the use of small molecular inhibitors that target specific steps of their biosynthesis pathways, especially in species in which no sterol biosynthesis mutants are available. The post-squalene part of the sterol biosynthesis diverged significantly between the three eukaryotic kingdoms (Supplementary Fig. S1): 1) Phytosterols derive from a 9β-19-cyclopropane ring precursor (cycloartenol), while animal and fungal sterols derive from lanosterol. 2) While many of the enzymatic conversions depend on diverged enzymatic isoforms, the sequence of removal of C-4 and C-14 methyl is different in plants compared to animals and fungi. 3) A plant-specific enzyme, CYCLOPROPYLSTEROL CYCLOISOMERASE (CPI) isomerizes the cyclopropane ring to produce Δ^8 phytosterol precursors. 4) Sterol side chains are methylated in plants and fungi (Rahier and Taton, 1997). Despite such important differences, plant sterol biosynthesis enzymes are able to complement yeast mutations in the corresponding enzyme (De Vriese *et al.*, 2021; Diener *et al.*, 2000; Kushiro *et al.*, 2001), suggesting the distinct metabolic precursors can still

dock the substrate binding pockets of these evolutionary distant enzymes. Consequently, sterol biosynthesis inhibitors that target specific sterol biosynthesis enzymes in fungi and mammals, often also inhibit the corresponding isoform in plants, albeit often with distinct efficiencies.

Azoles and morpholines represent two major classes of sterol biosynthesis inhibitors that act at distinct enzymatic conversions. Azoles typically target cytochrome P450 enzymes, including CYP51 that catalyzes sterol C-14 demethylation, but also other CYP-family members (Zhang *et al.*, 2002). A variety of imidazoles and 1,2,4-triazoles, such as paclobutrazole, voriconazole, have demonstrated effects on global sterol content in plants, associated with accumulation of C-14α methylated sterols (Burden *et al.*, 1987), indicating they inhibit CYP51 in plants. Some azoles were developed that selectively inhibit a subset of cytochrome P450s, leading to the development of azole fungicides, or plant growth regulators that are commonly used in agriculture and horticulture (Jørgensen and Heick, 2021). The triazoles paclobutrazole and uniconazole interfere with gibberellin biosynthesis by inhibiting CYP701 ent-kaurene oxidases, ABA biosynthesis by inhibiting CYP707 while brassinazole inhibits brassinosteroid biosynthesis.

Their use as antifungals in agriculture depends largely on affinity differences between isoforms of the different kingdoms. Voriconazole, a triazole-type fungicide, inhibits members of the CYP51 superfamily of 14α-demethylase cytochrome P450 enzymes in both yeast (0.2 μM) (Saravolatz *et al.*, 2003) and plants (1 μM) (Rozhon *et al.*, 2013). Notably, natural variation in CYP51 sequence explains variation in voriconazole sensitivity between different species (Rozhon *et al.*, 2013). Of these inhibitors, only fenpropimorph, a morpholine-derived fungicide, seems to be commonly used to manipulate sterol biosynthesis in plants. In yeast, fenpropimorph inhibits C-8,7 sterol isomerase (subnanomolar concentrations) and C-14 sterol reductase (micromolar concentrations) (Kerkenaar, 1990; Marcireau *et al.*, 1990). Also in plants, fenpropimorph inhibits the plant C14-reductase and C-8,7 sterol isomerase activities. Additionally, fenpropimorph also potently inhibits the plant-specific cyclopropyl-cycloisomerase (CPI) (Rahier *et al.*, 1986; Taton *et*

al., 1987). However, fenpropimorph and similar morpholines are commonly used in plants at concentrations that are multiple orders of magnitude higher (high micromolar range) than their effective concentration in yeast (Boutte *et al.*, 2010; He *et al.*, 2003; Li *et al.*, 2015).

Many enzymatic steps of cholesterol biosynthesis in animals are analogous to those of the yeast and plant biosynthesis pathway (Desmond and Gribaldo, 2009) (Supplementary Fig. S1). This explains why some inhibitors of human cholesterol biosynthesis and/or fungal lanosterol biosynthesis target analogous steps in phytosterol biosynthesis. Given the medicinal applications, the list of inhibitors that target different steps of human cholesterol biosynthesis is continually expanding (Kim *et al.*, 2016; Korade *et al.*, 2016). Since the current library of characterized plant sterol biosynthesis inhibitors is rather limited (De Vriese *et al.*, 2021), we set out to expand the current catalog of inhibitors. Therefore, we selected a subset of compounds that target different steps of the mammalian cholesterol biosynthesis pathway that were recently identified in screens in human cell systems (Table 1). Clotrimazole, bifonazole and econazole are anti-fungal imidazoles that are widely used in human and veterinary medicine. Of these imidazoles, clotrimazole was also reported to have deleterious effects on the monocotyledonous macrophytes *Lemna minor* and *Lemna gibba* (Dias de Santos Alkimin *et al.*, 2020), and different algae, correlated with shifts in sterol profiles (Porsbring *et al.*, 2009; Voshall *et al.*, 2021). Fluphenazine, perphenazine and trifluoperazine are phenothiazines that are widely used to treat psychoses and schizophrenia, possibly by antagonizing dopamine receptors. In plants, fluphenazine and trifluoperazine have been used as calmodulin inhibitors (Fujiki *et al.*, 2005). Trifluoperazine is reported to inhibit electron transport and ATP production in plant mitochondria, possibly independently of an effect on CaM (Dunn *et al.*, 1984). Clomiphene and tamoxifen are triphenylethylenes that are used for treatment of infertility and breast cancer based on their selective modulation of estrogen receptor activity, and are commonly referred to as Selective Estrogen Receptor Modulators (SERMs) (Haskell, 2003). Acitretin is a vitamin A-derivative that is

commonly used to treat psoriasis. Doxepin is a tricyclic antidepressant that increases serotonin and norepinephrine levels in the brain. Overall, none of the selected chemicals, even the imidazoles, are established as inhibitors of sterol biosynthesis in higher plants.

We provide proof-of-concept for several imidazoles as putative inhibitors of CYP51. Moreover, we identified the Selective Estrogen Receptor Modulator clomiphene as a novel inhibitor of plant sterol biosynthesis in part by inhibiting the plant-specific cyclopropyl-cycloisomerase CPI1. These findings illustrate the principle that the wide array of, often commercially available, animal sterol biosynthesis inhibitors can be exploited for the efficient identification of novel plant sterol biosynthesis inhibitors. The identified inhibitors expand the current toolbox for studying and manipulating the canonical sterol biosynthesis pathway in plants.

Materials and methods

Plant materials and growth conditions

Arabidopsis (*Arabidopsis thaliana* (L.) Heynh.) seeds were surface-sterilized for 15 min in 10% bleach, washed four times with sterile water and plated on ½-strength Murashige & Skoog medium (pH 5.7), with 0.5% sucrose, 0.8% agar. Plants were stratified at 4°C for 2 or 3 d in darkness and then transferred to a growth chamber at 21 °C under continuous illumination (light intensity 120 µmol m^{-2} s^{-1}). The Arabidopsis accession Columbia-0 (Col-0) was used as a WT for phenotypic screening and GC-MS profiling. Other assays were based on lines described previously, *ABCB19::ABCB19-GFP* (Wu *et al.*, 2007), 35S::AtCYP51-YFP (Rozhon *et al.*, 2013) *DR5rev::GFP* (Friml *et al.*, 2003), *yuc3,5,7,8,9* (Chen *et al.*, 2014) and *tir1 afb2* (Parry *et al.*, 2009).

Rice seeds (*Oryza sativa cv. Wuyungeng7*) were sterilized with 70% (v/v) ethanol for 1 min, followed by 30%(v/v) sodium hypochlorite solution for 30 min. Geminated rice seedlings were first grown in water for 3 days in a growth chamber at 24℃ under continuous illumination (light intensity 120μmol m^{-2} s^{-1}), and rice seedlings with 1.5 cm long seminal root (SR) were then transferred to the hydroponic culture supplemented with modified Kimura B solution for different inhibitor treatments. The modified Kimura B solution (pH 5.5, adjusted with HCl) contained 1.25mM $(NH4)_2SO_4$, 2.5mM KNO_3, 1mM $CaCl_2$, 0.3 mM KH_2PO_4, 0.35mM K_2SO_4, 1mM $MgSO_47H_2O$, 0.5mM $Na_2SiO_35H_2O$, 9μM $MnCl_24H_2O$, 0.39μM $Na_2MoO_42H_2O$, 20μM H_3BO_3, 0.77μM $ZnSO_47H_2O$, 0.32μM $CuSO_45H_2O$ and 20μM Fe(II)-EDTA. The rice seedlings were treated for 3 days unless otherwise noted and the hydroponic culture was refreshed every 2 days

Confocal microscopy

A Zeiss LSM 710 or Nikon A1 confocal microscope was used with a x20 objective with GFP was used to analyze ABCB19-GFP and DR5rev::GFP signals in the primary root meristem. Quantitative analyses of the GFP signals were performed using Fiji (Schindelin *et al.*, 2015).

Luminescence analysis

The luminescence emitted by the DR5::LUC plants was detected using charge-coupled device (CCD) cameras integrated either in Nightshade LB985 (Berthold Technologies, Bad Wildbad, Germany) imaging environment. To determine the effect of chemical inhibitors DR5::LUC luminescence, the seedlings were kept in total darkness for 10 min before imaging. Before imaging, the seedlings were transferred to new plates with or without chemical inhibiters and then were sprayed with 1 mM D-luciferin solution (d-Luciferin dissolved in 0.01% (v/v) Tween-

80 and 0.1% (v/v) DMSO; Duchefa Biochemie, Haarlem, the Netherlands). Luminescence was captured with an exposure time of 15 min. After imaging, the picture series were saved as 8-bit images in TIFF format for further analysis. Measurement of DR5::LUC signal intensities in the root was performed using Fiji.

Compounds

All compounds used in the experiments (acitretin, bifonazole, clomiphene, clotrimazole, doxepin, econazole, fluphenazine, flutrimazole, oxiconazole nitrate, perphenazine, tamoxifen, tetraphenylphosphonium, trifluoperazine, trityl chloride) were obtained from Sigma-Aldrich (Overijse, Belgium) and dissolved in DMSO.

Phenotype screen

Gas-sterilized *Arabidopsis thaliana* seeds (Col-0) were plated on ½ Murashige and Skoog (½ MS) medium supplemented with the appropriate compounds at various concentrations (3 rows/plate, 0.5 cm between seeds). For the primary root length experiments, the plated seeds were first stratified for 3 days in the dark at 4 °C and subsequently transferred to a growth chamber under continuous light conditions at 21 °C. After 7 days of growth, the plates were scanned and the primary root lengths of the seedlings were measured with Fiji (Schindelin *et al.*, 2015). For each treatment, 47-62 individual roots were measured. For the hypocotyl length experiments, the plated seeds were stratified for 3 days in the dark at 4 °C. To induce germination they were subjected to 4 hours light, prior to transfer to the dark. After 8 days of growth in the dark, the plates were scanned and the hypocotyl lengths of the seedlings were measured with ImageJ. For each treatment, 33-56 individual hypocotyls were measured.

GC-MS sterol profiling

Arabidopsis thaliana seeds were grown on ½ MS plates (no sucrose) for 3 days until germination. The seedlings were subsequently transferred to wells of 6-well plates containing 5 ml liquid ½ MS medium (no sucrose) and 0.5 or 5 µM of the appropriate compounds, or 0.1% DMSO (1 well per sample, 5 biological replicates per treatment). The seedlings were grown for 5 days in these wells with the compounds, after which they were frozen in liquid nitrogen and thoroughly ground into powder.

Approximately 100 mg (fresh weight) of plant material ground under liquid nitrogen was extracted with 1 mL of methanol to which 5 µg/mL of β-amyrin was added as internal standard. The extractions were carried out at room temperature for 30 min, after which the samples were centrifuged at 20,800 x g for 5 min. The supernatant was collected and evaporated to dryness under vacuum. The remaining plant material was lyophilized for dry weight determination. The samples were derivatized for GC-MS analysis by adding 10 µL of pyridine and 50 µL of N-Methyl-N-(trimethylsilyl)trifluoroacetamide (Sigma-Aldrich) to the residue. GC-MS analysis was carried out using a GC model 6890 and an MS model 5973 (Agilent). A 1 µL aliquot was injected in splitless mode into a VF-5ms capillary column (Varian CP9013, Agilent). The GC was operated at a constant helium flow of 1 mL per min and the injector was set to 280°C. The oven was held at 80 °C for 1 min after injection, then ramped to 280 °C at 20 °C per min, held at 280 °C for 30 min, ramped to 320 °C at 20 °C per min, held at 320 °C for one min, and finally cooled to 80 °C at 50 °C per min. The MS transfer line was set to 250 °C, the MS ion source to 230 °C, and the quadrupole to 150 °C, throughout. Full EI-MS (Electron Impact-MS) full scan spectra between *m/z* 60-800 were recorded after a solvent delay of 7.8 min. Peak areas were integrated using Masshunter Qualitative Analysis Software (Agilent) and normalized against the dry weight of the sample and the peak area of the internal standard. The total ion currents underneath the peaks corresponding to campesterol, stigmasterol, β-sitosterol, isofucosterol and the internal standard β-amyrin were determined for all samples. To correct for the loss of analyte during sample

preparation or analysis, the values for these three sterols were normalized against the internal standard β-amyrin, a pentacyclic triterpene alcohol with physicochemical properties similar to the profiled sterols. In addition, the obtained values were also corrected for the amount of plant material that was extracted by dividing the obtained values by the dry weight of the extracted plant material. The relative abundance of the phytosterols β-sitosterol, stigmasterol, campesterol and isofucosterol in the different treatments was calculated by normalization against the DMSO control.

Drug Affinity Responsive Target Stability (DARTS)

Seven-day-old CYP51G1-YFP *Arabidopsi*s seedlings were used for total protein extraction. The seedlings were ground in liquid nitrogen, resuspended in total protein extraction buffer (25 mM Tris-HCl, pH 7.5, 150 mM NaCl; 0.1% [v/v] IGEPAL CA-630, and Roche cOmplete ULTRA protease inhibitor cocktail, EDTA free) in a 1:2 (w/v) ratio, and centrifuged at 15,000 *g* to discard the cell debris. After determining the protein concentration with the Quick Start Bradford 1× Dye Reagent (Bio-Rad), the cell lysate was split into LoBind tubes and incubated with DMSO or Clot at a 20 µM concentration for 30 min at 4 °C with slow mixing. The treated protein extracts were further aliquoted, and each of the aliquots was mixed with Pronase (Roche) at the corresponding dilution prepared in pronase buffer (25 mM Tris-HCl, pH 7.5, and 150 mM NaCl) to achieve the aimed ratio of total enzyme to total protein substrate. After incubation for 30 min at room temperature, the proteolytic digestion was stopped by adding a protease inhibitor cocktail (Roche), and the tubes were incubated on ice for 10 min. The protein samples were then mixed with 4 × NuPAGE LDS sample buffer (Invitrogen) and 10 x NuPage reducing reagent (Invitrogen), heated at 70 °C for 10 min, and loaded onto 4-15% Mini-PROTEAN® TGX™ Precast Gels (Bio-Rad). The protein transfer to PVDF membranes was performed using the Trans-Blot® Turbo™ Rapid Transfer System (Bio-Rad) and the protein detection was done according to standard protein gel blotting procedures. The membranes were probed with α-GFP HRP-coupled (1:5000;

Miltenyi Biotec) and rabbit α-ATPβ (1:2000; Agrisera; reference for plant protein loading). The secondary antibodies were ECL α-rabbit IgG, horseradish peroxidase-linked whole antibody (GE Healthcare). Blots were developed with Western Lightning Plus-ECL, Enhanced Chemiluminescence Substrate (Perkin-Elmer), and imaged with the Bio-Rad ChemiDoc XRS+ molecular imager. Intensity of protein bands was measured with the Bio-Rad Image Lab software package. The ratio between the compound- and mock-treated samples for each of the pronase concentrations was calculated.

Statistical analysis

Statistical analyses were performed using GraphPad Prism 10.1.2. Details of sample size, replicates and statistical tests (two-tailed t-test, one-way ANOVA, two-way ANOVA and Tukey's multiple comparisons test) are stated in the corresponding legends.

Results

Hypocotyl and root phenotypes highlight putative phytosterol biosynthesis inhibitors among a set of cholesterol biosynthesis inhibitors

As an indirect readout of defective phytosterol biosynthesis (Rozhon *et al.*, 2013), we monitored the ability of the inhibitors to reduce hypocotyl length of etiolated Arabidopsis seedlings (Fig. 1A-E; Supplementary Fig. S2A). Bifonazole, clotrimazole and econazole strongly reduced hypocotyl length and were already effective at 0.5 µM concentrations (Fig. 1A,C,D). Clomiphene had an effect at higher concentrations (5 – 10 µM range) and tamoxifen reduced hypocotyl length only at 10 µM (Fig. 1B,C,E). Another putative C-8,7 isomerase/DHCR24 inhibitor, Perphenazine, as well as the DHCR24 inhibitors fluphenazine, acitretin, trifluoperazine and doxepin had no significant effects on hypocotyl elongation, even at the highest concentration (10 µM) tested (Fig.

1B and Supplementary Fig. S2A), suggesting that the latter are not effective inhibitors of phytosterol biosynthesis.

Next, we analyzed the effects of these inhibitors on root growth of light grown seedlings (Fig. 1F-J; Supplementary Fig. S2B). In comparison to seedlings grown in the presence of 0.1% DMSO, several of the selected compounds strongly inhibited root growth. At concentrations as low as 0.1 µM, clotrimazole reduced the primary root length by more than 50% compared to the control, while, bifonazole and econazole did so at 0.5 µM (Fig. 1F,H,I). Clomiphene and tamoxifen also strongly reduced the primary root length, albeit at higher concentrations (1 µM and above) than the tested imidazoles (Fig. 1G,H,J). At concentrations of 5 µM and higher, clotrimazole, clomiphene and tamoxifen caused severe reductions in primary root length. Consistently with the low bioactivity in the hypocotyl elongation assay, acitretin, doxepin, perphenazine, fluphenazine and trifluoperazine had no obvious effect on the primary root length at the highest tested concentration of 10 µM (Supplementary Fig. S2B). Due to the low bioactivity in our assays, we did not further pursue acitretin, doxepin, perphenazine, fluphenazine and trifluoperazine in the subsequent analyses.

To assess the time needed to cause root growth defects, seedlings were transferred after germination on normal medium to medium with 0.5 µM and 1 µM of the retained inhibitors (Supplementary Fig. S2C,D). Notably, all tested imidazoles (bifonazole, clotrimazole and econazole) yielded a rapid, near complete inhibition of root growth at 0.5 µM and 1 µM, corroborating their high bioactivity. The inhibitory effect of clomiphene was less prominent at these concentrations than for the imidazoles. The inhibition of tamoxifen on root growth could not be confirmed in the transfer experiment, and was therefore no longer considered in the following experiments. Lastly, we tested the effects of the remaining inhibitors on root growth in rice (Supplementary Fig. S2E,F). Each of the inhibitors reduced the root growth both concentrations,

with exception of econazole, inhibiting root growth only at 10 µM, indicating that rice root displays a differential sensitivity to these imidazoles.

Inhibitor induced cell division orientation defects and ectopic auxin accumulation

Defective sterol biosynthesis is often associated with defective cell division orientation, as is the case for *cpi1*, *fk* and *smt2smt3* double mutants (Jang *et al.*, 2000; Men *et al.*, 2008; Pullen *et al.*, 2010; Souter *et al.*, 2002). Therefore, we visualized the root meristem organization of inhibitor treated roots using ABCB19-GFP as a plasma membrane marker (Fig. 2A,B). We focused on the inhibitors that caused reductions in the root growth assays. The typical regular organization of the meristem was disrupted by all inhibitors, as indicated by the appearance of aberrant cell division orientations (Fig. 2A,B). While bifonazole, clomiphene, and econazole treatment potently disrupted cell division orientations in the root meristem, this was less obvious upon clotrimazole treatment (Fig. 2A). Similarly, cell division orientation defects were induced within 2 days of transfer to the inhibitors, and after 4 days the plasma membrane signal became diffuse for the azoles, but not for clomiphene (Supplementary Fig. S3A,B).

A second phenotype often seen in sterol biosynthesis mutants is an ectopic auxin accumulation in the lateral root cap (LRC) (Souter *et al.*, 2002; Wang *et al.*, 2021). Each of the tested inhibitors induced the spreading of the auxin response marker DR5rev::GFP. Instead of the typical restricted triangular expression maximum overlapping with the quiescence center and columella, the inhibitor treatment induced ectopic signals in the LRC with varying efficiencies (Fig. 2C,D). A similar ectopic DR5rev::GFP signal could be induced within 2 days of transfer (Supplementary Fig. S3C,D).

The ectopic auxin response signals in *cpi1-1* seems to involve induction of auxin biosynthesis (Wang *et al.*, 2021). Therefore, we asked if the effects on auxin biosynthesis could

explain the short root phenotype after inhibitor treatment. The *yuc3,5,7,8,9* quintuple (*yucQ*) mutant has strongly reduced root auxin levels and can be rescued by a nanomolar amount of auxin (Chen *et al.*, 2014). However, none of the inhibitors could rescue the root growth of *yucQ*. Instead, a similar relative root growth inhibition was seen as in WT (Supplementary Fig. S3E). Moreover, the auxin receptor double mutant *tir1afb2*, displayed a similar inhibitor sensitivity as WT (Supplementary Fig. S3E). This shows that the short root phenotype is probably not due to the ectopic auxin accumulation.

Jointly, the induced cell division orientation defects and ectopic DR5rev::GFP signals highlights bifonazole, clomiphene, clotrimazole and econazole as potential inhibitors of sterol biosynthesis.

GC-MS analysis reveals disturbed sterol composition in Arabidopsis seedlings after inhibitor treatment

Next, we determined the impact of the compounds on the sterol composition of Arabidopsis seedlings (Fig. 3). Seedlings were transferred for 5 days to liquid medium (without sucrose) containing 0.5 µM or 5 µM of bifonazole, clomiphene, clotrimazole and econazole. Sterols were extracted and analyzed via gas chromatography-mass spectrometry (GC-MS), using β-amyrin as an internal standard. The other major peaks in the GC-MS chromatograms corresponded to the three major phytosterols in Arabidopsis (campesterol, stigmasterol, and β-sitosterol), the sterol biosynthesis intermediate isofucosterol and α-tocopherol (vitamin E) (Fig. 3A). Structural characterization of these metabolites was conducted by matching their EI-MS spectra against NIST ’20 Mass Spectral Library (Supplementary Fig. S4).

From these analyses, it was clear that most of the tested compounds had at least some effect on the sterol composition of these three major phytosterols, and the β-sitosterol-precursor isofucosterol (Fig. 3B-E). All compounds strongly reduced the levels of isofucosterol (Fig. 3B), suggesting that these molecules have an impact on sterol biosynthesis upstream of isofucosterol. Consistently, the isofucosterol-derived sterols β-sitosterol and stigmasterol levels were also reduced (Fig. 3C,D). A similar, albeit weaker, trend was observed for campesterol, with exception of a slight increase for the 0.5 µM bifonazole treatment (Fig. 3E). Surprisingly, β-sitosterol levels in the clotrimazole samples were markedly less reduced than those of its direct product stigmasterol (Fig. 3D,E). This suggests that clotrimazole, in addition to its effects upstream of isofucosterol, might also reduce the flux from β-sitosterol to stigmasterol, rendering β-sitosterol levels less sensitive to inhibition of upstream steps.

Clotrimazole, bifonazole and econazole are inhibitors of CYP51 activity in Arabidopsis.

To infer the sterol biosynthesis step that is most likely targeted by these inhibitors, we revisited the TIC GC-MS full scan chromatograms for each treatment, in search of new peaks that likely correspond to sterol biosynthesis intermediates, and derivatives thereof. In the TIC GC-MS full scan chromatograms of all imidazole-treated samples, we observed the appearance of up to 4 new peaks, with metabolite 1 accumulating prominently in all imidazole treated samples (Fig. 4A; Supplementary Fig. S5A,B).

The GC-MS profiles of these metabolites displayed prominent ions at $[M\text{-}CH_3]^+$ and $[M\text{-}TMSiOH\text{-}CH_3]^+$ (Fig. 4B,C; Supplementary Fig. S6A,B), which are indicative of Δ^8 sterols with a 14α-methyl group (Goad and Akihisha, 1997). The accumulation of Δ^8 sterols with a 14α-methyl group is consistent with clotrimazole, bifonazole and econazole inhibiting 14α-demethylase activity in Arabidopsis (AtCYP51G1), a deeply conserved target of many azoles (Crowley and Gallagher, 2014; Lamb *et al.*, 2001). A NIST ’20 database search revealed that the GC-MS

spectrum of metabolite 4 matched with that of TMS-obtusifoliol (Fig. 4B), the preferred target of AtCYP51G1.

Similarities in the major ions suggest that the other three metabolites could be derivatives of obtusifoliol metabolites (Fig. 4 and Supplementary Fig. S6). Metabolite 1 was the major accumulating metabolite not only for clotrimazole, but also for bifonazole and econazole treatments (Fig. 4A, Supplementary Fig. S5A-B) and had an GC-MS spectrum that was also highly similar to that of TMS-obtusifoliol (NIST '20) (Fig. 4C). The major differences between both spectra were at the level of its molecular ion $[M]^+$, and the fragments $[M\text{-}CH_3]^+$ and $[M\text{-}TMSiOH\text{-}CH_3]^+$, all of which had an *m/z* value that was 12 Da lower than the corresponding ions in the GC-MS spectrum of TMS-obtusifoliol. This suggests that it contains one carbon atom less than obtusifoliol, yielding $C_{29}H_{50}O$ (TMS not counted). This chemical formula corresponds to that of 14α-methyl-24(24)-dihydrofecosterol, the major metabolite accumulating in *atcyp51g1* mutants (Kim *et al.*, 2005).

The biosynthesis of 14α-methyl-24(28)-dihydrofecosterol from obtusifoliol requires C4α-demethylation and C24(28) double bond reduction (Supplementary Fig. S5C). The C4α-demethylation of obtusifoliol was also seen in the *Atcyp51g1* mutant with the accumulation 14α-methyl-fecosterol ($C_{29}H_{48}O$) (Kim *et al.*, 2005). The molecular ion of metabolite 2, *m/z* 484 (Supplementary Fig. S6A), corresponds with a chemical formula of $C_{29}H_{48}O$ and a double bond equivalent (DBE) of 6, which indicates the presence of 2 double bonds. This metabolite could thus be 14α-methyl-fecosterol. Metabolite 3 displayed the molecular ion at *m*/*z* 500 (Supplementary Fig. S6B), matching a chemical formula of $C_{30}H_{52}O$ and a DBE of 5, indicating a single double bond. This corresponds to the main features of 24(24)-dihydro-obtusifoliol, another metabolite that also accumulates in the *cyp51* mutant (Kim *et al.*, 2005). Jointly, the accumulation of these 14α-methyl sterols indicates that clotrimazole, bifonazole and econazole inhibit CYP51 activity.

To validate whether the Arabidopsis CYP51 is a direct protein target of clotrimazole, we used the drug affinity-responsive target stability (DARTS) assay (Mishev *et al.*, 2018). This assay assumes that a protein's sensitivity to proteolytic degradation is altered upon drug binding. Lysates from Arabidopsis seedlings overexpressing ATCYP51G1-YFP (Rozhon *et al.*, 2013), were incubated with increasing concentrations of pronase, a mixture of proteases, in the presence or absence of clotrimazole. Subsequent quantification of the intact protein revealed a significant stabilization effect of clotrimazole on ATCYP51G1-YFP, but not on the unrelated endogenous ATP synthase β (Fig. 4D,E). Therefore, the DARTS experiments corroborate that clotrimazole can interact directly with CYP51G1. Together with the GC-MS analyses, these data show that clotrimazole is a direct inhibitor of CYP51G1 in Arabidopsis.

Clomiphene inhibits CPI activity in Arabidopsis

In contrast to the imidazole TIC GC-MS chromatograms, no 14α-methyl-24(28)-dihydrofecosterol (metabolite 1) peak appeared in the clomiphene chromatograms. Instead, five new compounds appeared in the clomiphene-treated samples that were not induced in the imidazole-treated samples (Fig. 5A; pink arrows), suggesting that clomiphene has a different target than the imidazoles. The GC-MS spectrum of the most prominent peak (metabolite 9), revealed a mixed spectrum, indicating the coelution of two metabolites (metabolites 9a and 9b). A database search of the deconvoluted spectra revealed that the GC-MS spectra for these metabolites corresponded to the fragmentation spectra of TMS-cycloeucalenol and TMS-α-amyrin (Fig. 5B,C).

Similarly to TMS-cycloeucalenol, metabolite 6 and metabolite 7 showed two intense fragment ions $[M\text{-}TMSiOH]^+$ and $[M\text{-}TMSiOH\text{-}CH_3]^+$, and a (very) weak molecular ion ($[M]^+$) (Supplementary Fig. S7A,B), indicating these metabolites are also 9β,19-cyclopropanesterols (Goad and Akihisha, 1997), related to cycloeucalenol. Based on the *m/z* of their molecular ions,

one is likely its demethylated version, 24-methylene pollinastanol (metabolite 6) and the other differing from the previous by a reduced double bond, 24-methyl pollinastanol (metabolite 7) (Supplementary Fig. S7A,B). The identity of these metabolites was further supported by a shared fragment ion at *m/z* 269, representing the sterol backbone ([M-TMSiOH-SC]$^+$) and a fragment ion unique to 24-methyl pollinastanol at *m/z* 220 (Böhme *et al.*, 1997). The accumulation of cycloeucalenol, and its aberrant metabolites 24-methylene pollinastanol and 24-methyl pollinastanol was also reported in the *cpi1-1* mutant (Men *et al.*, 2008), suggesting that clomiphene inhibits CYCLOPROPYLSTEROL CYCLOISOMERASE1 (CPI1) activity (Fig. 5D).

The GC-MS spectrum of metabolite 5 was very similar to that of 24-methylene lophenol ($C_{29}H_{48}O$) (Zu *et al.*, 2021), including major fragment ions (*m/z* 343, 255 and 229) (Supplementary Fig. S7C).This suggests that the structure of metabolite 5 is closely related to 24-methylene lophenol. The identity of metabolite 8 (Supplementary Fig. S7D) could not be reliably resolved due to low abundance, but also resembled the spectrum of 24-methylene lophenol. The accumulation of metabolites that are related to 24-methylene lophenol indicated that clomiphene might also target enzymes acting downstream of 24-methylene lophenol, such as SMO2 and SMT2/3.

Discussion

Phytosterol biosynthesis is orchestrated by complex, branched pathways that are regulated by a wide range of enzymes, which makes the study of these processes often difficult. While several mutants are available that are defective in specific steps of phytosterol biosynthesis, these mutants often show severe growth phenotypes and are thus not ideal to study sterol biosynthesis defects later in a plant's life. Notably, mutants are also unavailable for studying sterol biosynthesis in non-model species, making such studies largely reliant on sterol biosynthesis inhibitors. Unfortunately, the current toolset of sterol biosynthesis inhibitors in plants is limited (De

Vriese *et al.*, 2021). The close homology of the structures and the relative conservation of enzymes involved, explains why imidazoles that are known to block sterol biosynthesis in animals and/or fungi can also interfere with sterol biosynthesis in plants (He *et al.*, 2003; Rozhon *et al.*, 2013). While differences in structure and divergence of the catalytic centers may cause shifts in specificity, inhibitors of human sterol biosynthesis should thus be enriched in molecules that can interfere with plant sterol biosynthesis.

We exploited this principle by exploring a set of putative mammalian cholesterol biosynthesis inhibitors and identified several new inhibitors of plant sterol biosynthesis. Based on morphological and biochemical effects we demonstrate that the imidazoles, bifonazole, clotrimazole, and econazole, and the selective estrogen receptor modulator, clomiphene, are potent inhibitors of the canonical sterol biosynthesis pathway in plants. Matching the strong functional conservation of CYP51 activities, the tested imidazoles were found to potently interfere with CYP51G1 of Arabidopsis. This principle could not be applied for clomiphene. Instead of targeting the expected homologous enzymes with C8,7 isomerisation or C24-reductase activities, we found that clomiphene targeted CPI activities in Arabidopsis. Notably, multiple inhibitors of human sterol biosynthesis did not have strong effects on plant growth, indicating that they do not inhibit plant sterol biosynthesis, and were therefore not further analyzed.

Jointly, these data suggest that the exploration of inhibitors of human sterol biosynthesis is a valuable approach for identifying new inhibitors of plant sterol biosynthesis. Exploration of structural variants for improving affinity and specificity could lead to the development of plant-specific sterol biosynthesis inhibitors.

Bifonazole, clotrimazole and econazole are inhibitors of plant CYP51 activity

Multiple azoles were identified as potent fungicides by inhibiting the cytochrome P450-dependent monooxygenase CYP51 (Shafiei *et al.*, 2020). They typically act by non-competitive binding to the ferric ion of the heme group of the cytochrome P450, thus preventing substrate binding (Warrilow *et al.*, 2013). Sterol C14-demethylation is a highly conserved step in sterol biosynthesis in eukaryotes, and is mediated by CYP51 enzymes. The strong conservation of CYP51 enzymatic activity is also reflected in its broad sensitivity to different azoles (Shafiei *et al.*, 2020). Yet, sequence divergence between fungi, plants and animals has installed differential sensitivities to azoles, allowing their application as fungicides in medicine and agriculture. In example, bifonazole, clotrimazole, and econazole are commonly used to treat fungal infection of the skin and urogenital tracts, reflecting their preference towards fungal over human CYP51s (Warrilow *et al.*, 2013). We found that bifonazole, clotrimazole, and econazole interfered with plant growth and development, with effects already at submicromolar concentrations. Of these inhibitors only clotrimazole was previously shown to be bioactive in plants; it is toxic to Lemna species (Alkimin *et al.*, 2020), and it inhibits radish root growth (Bach, 1985), and root gravitropism in *Pisum sativum* (Amzallag and Vaisman, 2006). These studies did not provide biochemical evidence that sterol biosynthesis was indeed inhibited in these conditions. Our GC-MS analysis revealed that bifonazole, clotrimazole, and econazole treatments induce the accumulation of sterol biosynthesis intermediates that also accumulate in the Arabidopsis *cyp51* mutant (Kim *et al.*, 2005). Similarly, clotrimazole caused a lowering of the major sterols and accumulation of obtusifoliol in marine algae (Porsbring *et al.*, 2009). Moreover, our DARTS analyses demonstrated direct interaction between clotrimazole and AtCYP51, providing compelling evidence that clotrimazole likely directly inhibits CYP51 activities in plants. In extension it is thus also likely that bifonazole, and econazole directly inhibit the Arabidopsis CYP51 orthologue (CYP51G1).

Azoles may also have additional cytochrome P450 targets in the sterol biosynthesis pathway. In example, the conversion of β-sitosterol into stigmasterol is mediated by CYP710A sterol C22-desaturases. The additional inhibition of CYP710A could explain the high levels of β-

sitosterol compared to the prominent reduction of stigmasterol in the clotrimazole treated samples (Fig. 3C,D). The dual inhibition of C-14 demethylase (CYP51), and C-22 desaturase activity (CYP710A) was recently suggested for clotrimazole effects on the freshwater microalga *Chlorella sorokiniana* (Voshall *et al.*, 2021).

Clotrimazole was likely more potent than bifonazole and econazole in inhibiting CYP51 and CYP710A activities, as indicated by the more pronounced accumulation of obtusifoliol and derived aberrant sterols, and the less pronounced reduction of β-sitosterol. A consequence of the latter may be reflected in the modest effect of clotrimazole on cell division orientation compared to the other inhibitors (Fig. 2). This is in line with the observation that exogenously supplied β-sitosterol could recover abnormal lateral root development in *smt2smt3* mutants (Nakamoto *et al.*, 2015). Jointly, these data highlight clotrimazole, bifonazole and econazole as potent inhibitors of plant sterol biosynthesis, acting directly on CYP51 and possibly also on CYP710.

Clomiphene is a novel plant sterol biosynthesis inhibitor

Clomiphene is well known as estrogen receptor agonist or antagonist, depending on the target tissue, and is used to induce ovulation or treat breast cancer. In a repurposing screen of FDA (US Food and Drug Administration) approved drugs, clomiphene was identified as an inhibitor of Δ8-7 sterol isomerase and DHCR24 activities (Korade *et al.*, 2016). The corresponding enzymes in plants are the Δ8-7 sterol isomerase HYDRA1, and the C24 sterol side chain reductase DWARF1. Consistently with inhibition of sterol biosynthesis enzymes, clomiphene caused altered cell division patterns in the root meristem that were associated with reduced sterol levels. Unexpectedly, the analysis of the sterol biosynthesis intermediates indicated that clomiphene interferes with cyclopropylsterol-cycloisomerase (CPI), and possibly another step downstream of 24-methylene lophenol.

Current CPI pharmacology consists of morpholines such as fenpropimorph (Taton *et al.*, 1987), and LDAO (Darnet *et al.*, 2020). Similarly to clomiphene, neither inhibitor is selective for CPI. Morpholines additionally inhibit the C14 sterol reductase (FACKLE) and Δ8-7 sterol isomerase (HYDRA1) activities (Taton *et al.*, 1987), while LDAO is a potent inhibitor of 2,3-oxidosqualene cyclization to cycloartenol and β-amyrin (Cerutti *et al.*, 1985). Clomiphene caused the accumulation of two other metabolites. These metabolites seem related to 24-methylene lophenol, suggesting that clomiphene also targets downstream enzymes such as SMO2 and SMT2/3.

In human liver microsomes, nine clomiphene metabolites could be identified that were more potent estrogen antagonists than clomiphene itself (Mürdter *et al.*, 2012). It is therefore not unlikely that clomiphene is also metabolized in plants, and that one or more of these metabolites inhibit one or more steps of plant sterol biosynthesis. A more detailed exploration of clomiphene metabolism in plants will be required. Interestingly, CPI is a plant-specific enzyme (Desmond and Gribaldo, 2009), indicating that it is an interesting target for developing novel herbicides.

A call for caution for using estradiol and SERM-inducible systems

Our analyses identified clomiphene, a Selective Estradiol Receptor Modulator (SERM), as an inhibitor of sterol biosynthesis in plants. Clomiphene caused aberrant cell divisions in the root meristem. Similar cell division phenotypes were observed with tamoxifen, that can be metabolized in human cells into the SERM, 4-hydroxytamoxifen. This suggests that estrogen receptor ligands potentially inhibit sterol biosynthesis in plants.

Several systems that are commonly used for chemically induced expression in plants use estradiol or 4-hydroxytamoxifen as an activating ligand. The most popular system involves the chimeric transcription factor XVE, that can activate a LexA operator based promoter in response

to β-estradiol (Zuo *et al.*, 2000), that is typically applied between 2 and 10 μM in Arabidopsis (Schlucking *et al.*, 2013; Wang *et al.*, 2020; Yamada *et al.*, 2020), and up to 20 μM in rice protoplasts (Chen *et al.*, 2017). A derivative hereof allows for activation of UAS operator based promoters in response to the SERM 4-hydroxytamoxifen (Friml *et al.*, 2004), that is typically applied at 2 μM in Arabidopsis (Kitakura *et al.*, 2011). The concentrations of these ligands are in the range of, and even higher than, those at which we observed significant root growth phenotypes for clomiphene and tamoxifen, molecules whose chemical space closely matches that of the inductive ligands, β-estradiol and 4-hydroxytamoxifen, respectively. This indicates that some of the observed phenotypes in such inducible backgrounds may be modified by reduced sterol content, or the accumulation of sterol biosynthesis intermediates. This calls for caution for using such inducible systems in the context of cell biological processes that are sterol-dependent, such as clathrin-mediated endocytosis (Men *et al.*, 2008), cytokinesis (Boutte *et al.*, 2010; Nakamoto *et al.*, 2015) and polarity (Men *et al.*, 2008; Stanislas *et al.*, 2015).

Supplementary data

Supplementary Fig. S1. Scheme of sterol biosynthesis in fungi, animals and plants

Supplementary Fig. S2 Additional dose responses, transfer experiments and effects on rice roots

Supplementary Fig. S3 Root responses to short-term inhibitors treatment.

Supplementary Fig. S4 Molecular identification of major sterols via GC-MS

Supplementary Fig. S5 Bifonazole and econazole induce accumulation of metabolite 1

Supplementary Fig. S6 GC-MS spectra of metabolite 2 and 3

Supplementary Fig. S7 GC-MS spectra of metabolites 5, 6, 7, 8

Acknowledgments

This work was performed in collaboration with the VIB Metabolomics Core

Author Contributions

TB and SV: Conceptualization; TB and SV: Data curation; Q.W., KDV, SS, SD, JP, QL and SV Formal analysis; Q.W., KDV, SD, JP and QL: Investigation; TB and SV Project administration; QW, KDV and GG Resources; WV, AG, GG, ER, DG, TB and SV: Supervision; QW, SD, SS: Validation; QW, KDV, RW, ML, QQL, QL, SD and SV: Visualization; QW, KDV, SD, TB and SV: Writing-original draft; SD, AG, ER, DG, WV and TB Writing-review & editing

Conflict of interest

No conflict of interest is declared

Funding

This work was supported by the VIB Innovation Fund, and Fonds Wetenschappelijk Onderzoek Vlaanderen (G001221N and G049622N to SV), and the Chinese Scholarship Council (201808320431 to QW 201506220143 to QL)

Data availability

All data that was used in the manuscript is available from the authors upon request.

References

Alkimin GD, Santos J, Soares A, Nunes B. 2020. Ecotoxicological effects of the azole antifungal agent clotrimazole on the macrophyte species *Lemna minor* and *Lemna gibba*. Comparative Biochemistry and Physiology Part C: Toxicology & Pharmacology **237**, 108835.

Amzallag GN, Vaisman J. 2006. Influence of brassinosteroids on initiation of the root gravitropic response in Pisum sativum seedlings. Biologia Plantarum **50**, 283–286.

Azpiroz R, Wu Y, LoCascio JC, Feldmann KA. 1998. An Arabidopsis brassinosteroid-dependent mutant is blocked in cell elongation. The Plant Cell **10**, 219-230.

Bach TJ. 1985. Selected natural and synthetic enzyme inhibitors of sterol biosynthesis as molecular probes for in vivo studies concerning the regulation of plant growth. Plant Science **39**, 183-187.

Böhme F, Schmidt J, Van Sung, Adam G. 1997. 24-Metylepollinastanone, related triterpenoids and sterols from *Costus tonkinensis*. Phytochemistry **45**, 1041-1044.

Boutte Y, Frescatada-Rosa M, Men S, Chow CM, Ebine K, Gustavsson A, Johansson L, Ueda T, Moore I, Jurgens G, Grebe M. 2010. Endocytosis restricts Arabidopsis KNOLLE syntaxin to the cell division plane during late cytokinesis. EMBO Journal **29**, 546-558.

Boutte Y, Grebe M. 2009. Cellular processes relying on sterol function in plants. Current Opinion in Plant Biology **12**, 705-713.

Burden RS, Clark T, Holloway PJ. 1987. Effects of sterol biosynthesis-inhibiting fungicides and plant growth regulators on the sterol composition of barley plants. Pesticide Biochemistry and Physiology **27**, 289-300.

Cacas JL, Furt F, Le Guedard M, Schmitter JM, Bure C, Gerbeau-Pissot P, Moreau P, Bessoule JJ, Simon-Plas F, Mongrand S. 2012. Lipids of plant membrane rafts. Progress in Lipid Research **51**, 272-299.

Carland F, Fujioka S, Nelson T. 2010. The sterol methyltransferases SMT1, SMT2, and SMT3 influence Arabidopsis development through nonbrassinosteroid products. Plant Physiology **153**, 741-756.

Carland FM, Fujioka S, Takatsuto S, Yoshida S, Nelson T. 2002. The identification of CVP1 reveals a role for sterols in vascular patterning. The Plant Cell **14**, 2045-2058.

Catterou M, Dubois F, Schaller H, Aubanelle L, Vilcot B, Sangwan-Norreel BS, Sangwan RS. 2001. Brassinosteroids, microtubules and cell elongation in Arabidopsis thaliana. I. Molecular, cellular and physiological characterization of the Arabidopsis bull mutant, defective in the delta 7-sterol-C5-desaturation step leading to brassinosteroid biosynthesis. Planta **212**, 659-672.

Cerutti M, Delprino L, Cattel L, Bouviernave P, Duriatti A, Schuber F, Benveniste P. 1985. *N*-Oxide as a Potential Function in the Design of Enzyme-Inhibitors-Application to 2,3-Epoxysqualene-Sterol Cyclases. Journal of the Chemical Society, Chemical Communications **15**, 1054–1055.

Chen L-L, Wang G-Z, Zhang H-Y. 2007. Sterol biosynthesis and prokaryotes-to-eukaryotes evolution. Biochemical and Biophysical Research Communications **363**, 885-888.

Chen Q, Dai X, De-Paoli H, Cheng Y, Takebayashi Y, Kasahara H, Kamiya Y, Zhao Y. 2014. Auxin overproduction in shoots cannot rescue auxin deficiencies in Arabidopsis roots. Plant Cell Physiology **55**, 1072-1079.

Chen Z, Cheng Q, Hu C, Guo X, Chen Z, Lin Y, Hu T, Bellizzi M, Lu G, Wang GL, Wang Z, Chen S, Wang F. 2017. A Chemical-Induced, Seed-Soaking Activation Procedure for Regulated Gene Expression in Rice. Frontiers in Plant Science **8**, 1447.

Choe S, Dilkes BP, Gregory BD, Ross AS, Yuan H, Noguchi T, Fujioka S, Takatsuto S, Tanaka A, Yoshida S, Tax FE, Feldmann KA. 1999a. The Arabidopsis dwarf1 mutant is defective in the conversion of 24-methylenecholesterol to campesterol in brassinosteroid biosynthesis. Plant Physiology **119**, 897-907.

Choe S, Noguchi T, Fujioka S, Takatsuto S, Tissier CP, Gregory BD, Ross AS, Tanaka A, Yoshida S, Tax FE, Feldmann KA. 1999b. The Arabidopsis dwf7/ste1 mutant is defective in the delta7 sterol C-5 desaturation step leading to brassinosteroid biosynthesis. The Plant Cell **11**, 207-221.

Choe S, Tanaka A, Noguchi T, Fujioka S, Takatsuto S, Ross AS, Tax FE, Yoshida S, Feldmann KA. 2000. Lesions in the sterol delta reductase gene of Arabidopsis cause dwarfism due to a block in brassinosteroid biosynthesis. Plant Journal **21**, 431-443.

Clouse SD. 2000. Plant development: A role for sterols in embryogenesis. Current biology **10**, R601-604.
Crowley PD, Gallagher HC. 2014. Clotrimazole as a pharmaceutical: past, present and future. Journal of Applied Microbiology **117**, 611-617.

Darnet S, Blary A, Chevalier Q, Schaller H. 2021. Phytosterol Profiles, Genomes and Enzymes - An Overview. Frontiers in Plant Science **12**, 665206.

Darnet S, Martin LBB, Mercier P, Bracher F, Geoffroy P, Schaller H. 2020. Inhibition of Phytosterol Biosynthesis by Azasterols. Molecules **25**.

De Vriese K, Pollier J, Goossens A, Beeckman T, Vanneste S. 2021. Dissecting cholesterol and phytosterol biosynthesis via mutants and inhibitors. Journal of Experimental Botany **72**, 241-253.

Der C, Courty PE, Recorbet G, Wipf D, Simon-Plas F, Gerbeau-Pissot P. 2024. Sterols, pleiotropic players in plant-microbe interactions. Trends in Plant Science **29**, 524-534.

Desmond E, Gribaldo S. 2009. Phylogenomics of sterol synthesis: insights into the origin, evolution, and diversity of a key eukaryotic feature. Genome Biology and Evolution **1**, 364-381.

Dias de Santos Alkimin GJ, M. SAMV, Bruno N. 2020. Ecotoxicological effects of the azole antifungal agent clotrimazole on the macrophyte species *Lemna minor* and *Lemna gibba*. Comparative Biochemistry and Physiology Part C: Toxicology & Pharmacology **237**, 108835.

Diener AC, Li H, Zhou W, Whoriskey WJ, Nes WD, Fink GR. 2000. Sterol methyltransferase 1 controls the level of cholesterol in plants. The Plant Cell **12**, 853-870.

Dunn PPJ, Slabas AR, Cottingham IR, Moore AL. 1984. Trifluoperazine inhibition of electron transport and adenosine triphosphatase in plant mitochondria. Archives of Biochemistry and Biophysics **229**, 287-294.

Elsaman H, Golubtsov E, Brazil S, Ng N, Klugherz I, Martin R, Dichtl K, Müller C, Wagener J. 2024. Toxic eburicol accumulation drives the antifungal activity of azoles against Aspergillus fumigatus. Nature Communications **15**, 6312.

Friml J, Vieten A, Sauer M, Weijers D, Schwarz H, Hamann T, Offringa R, Jurgens G. 2003. Efflux-dependent auxin gradients establish the apical-basal axis of Arabidopsis. Nature **426**, 147-153.

Friml J, Yang X, Michniewicz M, Weijers D, Quint A, Tietz O, Benjamins R, Ouwerkerk PB, Ljung K, Sandberg G, Hooykaas PJ, Palme K, Offringa R. 2004. A PINOID-dependent binary switch in apical-basal PIN polar targeting directs auxin efflux. Science **306**, 862-865.

Fujiki Y, Nakagawa Y, Furumoto T, Yoshida S, Biswal B, Ito M, Watanabe A, Nishida I. 2005. Response to Darkness of Late-Responsive Dark-Inducible Genes is Positively Regulated by Leaf Age and Negatively Regulated by Calmodulin-Antagonist-Sensitive Signalling in Arabidopsis thaliana. Plant and Cell Physiology **46**, 1741-1746.

Goad LJ, Akihisha T. 1997. Mass spectrometry of sterols. In: Goad LJ, Akihisha T, eds. *Analysis of sterols*. Dordrecht: Springer, 152-196.

Gronnier J, Crowet J-M, Habenstein B, Nasir MN, Bayle V, Hosy E, Platre MP, Gouguet P, Raffaele S, Martinez D, Grelard A, Loquet A, Simon-Plas F, Gerbeau-Pissot P, Der C, Bayer EM, Jaillais Y, Deleu M, Germain V, Lins L, Mongrand S. 2017. Structural basis for plant plasma membrane protein dynamics and organization into functional nanodomains. Elife **6**, e26404.

Guo DA, Venkatramesh M, Nes WD. 1995. Developmental regulation of sterol biosynthesis in Zea mays. Lipids **30**, 203-219.

Han PP, Zhou J, Yuan YJ. 2009. Analysis of phospholipids, sterols, and fatty acids in Taxus chinensis var. mairei cells in response to shear stress. Biotechnology and applied biochemistry **54**, 105-112.

Hase Y, Fujioka S, Yoshida S, Sun G, Umeda M, Tanaka A. 2005. Ectopic endoreduplication caused by sterol alteration results in serrated petals in Arabidopsis. Journal of Experimental Botany **56**, 1263-1268.
Haskell SG. 2003. Selective estrogen receptor modulators. Southern Medical Journal **96**, 469-476.

He JX, Fujioka S, Li TC, Kang SG, Seto H, Takatsuto S, Yoshida S, Jang JC. 2003. Sterols regulate development and gene expression in Arabidopsis. Plant Physiology **131**, 1258-1269.

He Z, Wang ZY, Li J, Zhu Q, Lamb C, Ronald P, Chory J. 2000. Perception of brassinosteroids by the extracellular domain of the receptor kinase BRI1. Science (New York, N.Y.) **288**, 2360-2363.

Jang JC, Fujioka S, Tasaka M, Seto H, Takatsuto S, Ishii A, Aida M, Yoshida S, Sheen J. 2000. A critical role of sterols in embryonic patterning and meristem programming revealed by the fackel mutants of Arabidopsis thaliana. Genes & Development **14**, 1485-1497.

Jørgensen LN, Heick TM. 2021. Azole Use in Agriculture, Horticulture, and Wood Preservation - Is It Indispensable? Frontiers in Cellular and Infection Microbiology **11**, 730297.

Kerkenaar A. 1990. Inhibition of the sterol delta 14-reductase and delta 8-delta 7-isomerase in fungi. Biochemical Society Transactions **18**, 59-61.

Kim HB, Schaller H, Goh CH, Kwon M, Choe S, An CS, Durst F, Feldmann KA, Feyereisen R. 2005. Arabidopsis cyp51 mutant shows postembryonic seedling lethality associated with lack of membrane integrity. Plant Physiology **138**, 2033-2047.

Kim HY, Korade Z, Tallman KA, Liu W, Weaver CD, Mirnics K, Porter NA. 2016. Inhibitors of 7-Dehydrocholesterol Reductase: Screening of a Collection of Pharmacologically Active Compounds in Neuro2a Cells. Chemical research in toxicology **29**, 892-900.

Kitakura S, Vanneste S, Robert S, Löfke C, Teichmann T, Tanaka H, Friml J. 2011. Clathrin mediates endocytosis and polar distribution of PIN auxin transporters in Arabidopsis. The Plant Cell **23**, 1920-1931.

Klahre U, Noguchi T, Fujioka S, Takatsuto S, Yokota T, Nomura T, Yoshida S, Chua NH. 1998. The Arabidopsis DIMINUTO/DWARF1 gene encodes a protein involved in steroid synthesis. The Plant Cell **10**, 1677-1690.

Konopka CA, Backues SK, Bednarek SY. 2008. Dynamics of Arabidopsis dynamin-related protein 1C and a clathrin light chain at the plasma membrane. The Plant Cell **20**, 1363-1380.

Korade Z, Kim HY, Tallman KA, Liu W, Koczok K, Balogh I, Xu L, Mirnics K, Porter NA. 2016. The Effect of Small Molecules on Sterol Homeostasis: Measuring 7-Dehydrocholesterol in Dhcr7-Deficient Neuro2a Cells and Human Fibroblasts. Journal of medicinal chemistry **59**, 1102-1115.

Kumar MS, Ali K, Dahuja A, Tyagi A. 2015. Role of phytosterols in drought stress tolerance in rice. Plant physiology and biochemistry **96**, 83-89.

Kushiro M, Nakano T, Sato K, Yamagishi K, Asami T, Nakano A, Takatsuto S, Fujioka S, Ebizuka Y, Yoshida S. 2001. Obtusifoliol 14alpha-demethylase (CYP51) antisense Arabidopsis shows slow growth and long life. Biochemical and Biophysical Research Communications **285**, 98-104.

Lamb DC, Cannieux M, Warrilow AG, Bak S, Kahn RA, Manning NJ, Kelly DE, Kelly SL. 2001. Plant sterol 14 alpha-demethylase affinity for azole fungicides. Biochemical and Biophysical Research Communications **284**, 845-849.

Li R, Sun R, Hicks GR, Raikhel NV. 2015. Arabidopsis ribosomal proteins control vacuole trafficking and developmental programs through the regulation of lipid metabolism. Proceedings of the National Academy of Sciences of the United States of America **112**, E89-98.

Marcireau C, Guilloton M, Karst F. 1990. In vivo effects of fenpropimorph on the yeast Saccharomyces cerevisiae and determination of the molecular basis of the antifungal property. Antimicrobial agents and chemotherapy **34**, 989-993.

Men S, Boutte Y, Ikeda Y, Li X, Palme K, Stierhof YD, Hartmann MA, Moritz T, Grebe M. 2008. Sterol-dependent endocytosis mediates post-cytokinetic acquisition of PIN2 auxin efflux carrier polarity. Nature cell biology **10**, 237-244.

Mialoundama AS, Jadid N, Brunel J, Di Pascoli T, Heintz D, Erhardt M, Mutterer J, Bergdoll M, Ayoub D, Van Dorsselaer A, Rahier A, Nkeng P, Geoffroy P, Miesch M, Camara B, Bouvier F. 2013. Arabidopsis ERG28 Tethers the Sterol C4-Demethylation Complex to Prevent Accumulation of a Biosynthetic Intermediate That Interferes with Polar Auxin Transport The Plant Cell **25**, 4879-4893.

Mishev K, Lu Q, Denoo B, Peurois F, Dejonghe W, Hullaert J, De Rycke R, Boeren S, Bretou M, De Munck S, Sharma I, Goodman K, Kalinowska K, Storme V, Nguyen LSL, Drozdzecki A, Martins S, Nerinckx W, Audenaert D, Vert G, Madder A, Otegui MS, Isono E, Savvides SN, Annaert W, De Vries S, Cherfils J, Winne J, Russinova E. 2018. Nonselective Chemical Inhibition of Sec7 Domain-Containing ARF GTPase Exchange Factors. The Plant Cell **30**, 2573-2593.

Morales-Cedillo F, González-Solís A, Gutiérrez-Angoa L, Cano-Ramírez DL, Gavilanes-Ruiz M. 2015. Plant lipid environment and membrane enzymes: the case of the plasma membrane H+-ATPase. The Plant Cell Reports **34**, 617-629.

Moreau RA, Nyström L, Whitaker BD, Winkler-Moser JK, Baer DJ, Gebauer SK, Hicks KB. 2018. Phytosterols and their derivatives: Structural diversity, distribution, metabolism, analysis, and health-promoting uses. Progress in Lipid Research **70**, 35-61.

Mürdter TE, Kerb R, Turpeinen M, Schroth W, Ganchev B, Bohmer GM, Igel S, Schaeffeler E, Zanger U, Brauch H, Schwab M. 2012. Genetic polymorphism of cytochrome P450 2D6 determines oestrogen receptor activity of the major infertility drug clomiphene via its active metabolites. Human Molecular Genetics **21**, 1145-1154.

Nakamoto M, Schmit AC, Heintz D, Schaller H, Ohta D. 2015. Diversification of sterol methyltransferase enzymes in plants and a role for beta-sitosterol in oriented cell plate formation and polarized growth. Plant Journal **84**, 860-874.

Pan J, Fujioka S, Peng J, Chen J, Li G, Chen R. 2009. The E3 ubiquitin ligase SCFTIR1/AFB and membrane sterols play key roles in auxin regulation of endocytosis, recycling, and plasma membrane accumulation of the auxin efflux transporter PIN2 in Arabidopsis thaliana. The Plant Cell **21**, 568-580.

Parry G, Calderon-Villalobos LI, Prigge M, Peret B, Dharmasiri S, Itoh H, Lechner E, Gray WM, Bennett M, Estelle M. 2009. Complex regulation of the TIR1/AFB family of auxin receptors. Proceedings of the National Academy of Sciences of the United States of America **106**, 22540-22545.

Porsbring T, Blanck H, Tjellström H, Backhaus T. 2009. Toxicity of the pharmaceutical clotrimazole to marine microalgal communities. Aquatic Toxicology **91**, 203-211.

Pose D, Castanedo I, Borsani O, Nieto B, Rosado A, Taconnat L, Ferrer A, Dolan L, Valpuesta V, Botella MA. 2009. Identification of the Arabidopsis dry2/sqe1-5 mutant reveals a central role for sterols in drought tolerance and regulation of reactive oxygen species. The Plant journal **59**, 63-76.

Pullen M, Clark N, Zarinkamar F, Topping J, Lindsey K. 2010. Analysis of vascular development in the hydra sterol biosynthetic mutants of Arabidopsis. PLoS One **5**, e12227.

Rahier A, Schmitt P, Huss B, Benveniste P, Pommer EH. 1986. Chemical-Structure Activity Relationships of the Inhibition of Sterol Biosynthesis by N-Substituted Morpholines in Higher-Plants. Pesticide Biochemistry and Physiology **25**, 112-124.

Rahier A, Taton M. 1997. Fungicides as Tools in Studying Postsqualene Sterol Synthesis in Plants. Pesticide Biochemistry and Physiology **57**, 1-27.

Rozhon W, Husar S, Kalaivanan F, Khan M, Idlhammer M, Shumilina D, Lange T, Hoffmann T, Schwab W, Fujioka S, Poppenberger B. 2013. Genetic variation in plant CYP51s confers resistance against voriconazole, a novel inhibitor of brassinosteroid-dependent sterol biosynthesis. PloS one **8**, e53650.

Saravolatz LD, Johnson LB, Kauffman CA. 2003. Voriconazole: a new triazole antifungal agent. Clinical Infectious Diseases **36**, 630-637.

Schaller H. 2003. The role of sterols in plant growth and development. Progress in lipid research **42**, 163-175.

Schindelin J, Rueden CT, Hiner MC, Eliceiri KW. 2015. The ImageJ ecosystem: An open platform for biomedical image analysis. Molecular Reproduction and Development **82**, 518-529.

Schlucking K, Edel KH, Koster P, Drerup MM, Eckert C, Steinhorst L, Waadt R, Batistic O, Kudla J. 2013. A new beta-estradiol-inducible vector set that facilitates easy construction and efficient expression of transgenes reveals CBL3-dependent cytoplasm to tonoplast translocation of CIPK5. Molecular Plant **6**, 1814-1829.

Schrick K, Fujioka S, Takatsuto S, Stierhof YD, Stransky H, Yoshida S, Jürgens G. 2004. A link between sterol biosynthesis, the cell wall, and cellulose in Arabidopsis. Plant Joural **38**, 227-243.

Senthil-Kumar M, Wang K, Mysore KS. 2013. AtCYP710A1 gene-mediated stigmasterol production plays a role in imparting temperature stress tolerance in Arabidopsis thaliana. Plant signaling & behavior **8**, e23142.

Shafiei M, Peyton L, Hashemzadeh M, Foroumadi A. 2020. History of the development of antifungal azoles: A review on structures, SAR, and mechanism of action. Bioorganic Chemistry **104**, 104240.

Simon-Plas F, Perraki A, Bayer E, Gerbeau-Pissot P, Mongrand S. 2011. An update on plant membrane rafts. Current Opinion in Plant Biology **14**, 642-649.

Sonawane PD, Pollier J, Panda S, Szymanski J, Massalha H, Yona M, Unger T, Malitsky S, Arendt P, Pauwels L, Almekias-Siegl E, Rogachev I, Meir S, Cárdenas PD, Masri A, Petrikov M, Schaller H, Schaffer AA, Kamble A, Giri AP, Goossens A, Aharoni A. 2016. Plant cholesterol biosynthetic pathway overlaps with phytosterol metabolism. Nature Plants **3**, 16205.

Song J, Sun S, Ren H, Grison M, Boutté Y, Bai W, Men S. 2019. The SMO1 Family of Sterol 4α-Methyl Oxidases Is Essential for Auxin- and Cytokinin-Regulated Embryogenesis1. Plant Physiology **181**, 578-594.

Souter M, Topping J, Pullen M, Friml J, Palme K, Hackett R, Grierson D, Lindsey K. 2002. hydra Mutants of Arabidopsis are defective in sterol profiles and auxin and ethylene signaling. The Plant cell **14**, 1017-1031.

Stanislas T, Huser A, Barbosa IC, Kiefer CS, Brackmann K, Pietra S, Gustavsson A, Zourelidou M, Schwechheimer C, Grebe M. 2015. Arabidopsis D6PK is a lipid domain-dependent mediator of root epidermal planar polarity. Nature Plants **1**, 15162.

Taton M, Benveniste P, Rahier A. 1987. Mechanism of inhibition of sterol biosynthesis enzymes by *N*-substituted morpholines. Pesticide Science **21**, 269-280.

Voshall A, Christie NTM, Rose SL, Khasin M, Van Etten JL, Markham JE, Riekhof WR, Nickerson KW. 2021. Sterol Biosynthesis in Four Green Algae: A Bioinformatic Analysis of the Ergosterol Versus Phytosterol Decision Point. Journal of Phycology **57**, 1199-1211.

Wang M, Li P, Ma Y, Nie X, Grebe M, Men S. 2021. Membrane Sterol Composition in Arabidopsis thaliana Affects Root Elongation via Auxin Biosynthesis. International Journal of Molecular Sciences **22**.

Wang X, Ye L, Lyu M, Ursache R, Loytynoja A, Mahonen AP. 2020. An inducible genome editing system for plants. Nature Plants **6**, 766-772.

Warrilow AG, Parker JE, Kelly DE, Kelly SL. 2013. Azole affinity of sterol 14alpha-demethylase (CYP51) enzymes from *Candida albicans* and *Homo sapiens*. Antimicrobial Agents and Chemotherapy **57**, 1352-1360.

Willemsen V, Friml J, Grebe M, van den Toorn A, Palme K, Scheres B. 2003. Cell polarity and PIN protein positioning in Arabidopsis require STEROL METHYLTRANSFERASE1 function. The Plant cell **15**, 612-625.

Wu G, Lewis DR, Spalding EP. 2007. Mutations in Arabidopsis multidrug resistance-like ABC transporters separate the roles of acropetal and basipetal auxin transport in lateral root development. The Plant Cell **19**, 1826-1837.

Yamada M, Han X, Benfey PN. 2020. RGF1 controls root meristem size through ROS signalling. Nature **577**, 85-88.

Yang H, Richter GL, Wang X, Mlodzinska E, Carraro N, Ma G, Jenness M, Chao DY, Peer WA, Murphy AS. 2013. Sterols and sphingolipids differentially function in trafficking of the Arabidopsis ABCB19 auxin transporter. The Plant journal **74**, 37-47.

Yu L, Fan J, Zhou C, Xu C. 2021. Sterols are required for the coordinated assembly of lipid droplets in developing seeds. Nature Communications **12**, 5598.

Zhang W, Ramamoorthy Y, Kilicarslan T, Nolte H, Tyndale RF, Sellers EM. 2002. Inhibition of Cytochromes P450 by Antifungal Imidazole Derivatives. Drug Metabolism and Disposition **30**, 314.

Zhang X, Sun S, Nie X, Boutté Y, Grison M, Li P, Kuang S, Men S. 2016. Sterol Methyl Oxidases Affect Embryo Development via Auxin-Associated Mechanisms. Plant Physiology **171**, 468-482.

Zhao H, Ma B, Duan K-X, Li X-K, Lu X, Yin C-C, Tao J-J, Wei W, Zhang W-K, Xin P-Y, Man Lam S, Chu J-F, Shui G-H, Chen S-Y, Zhang J-S. 2020. The GDSL Lipase MHZ11 Modulates Ethylene Signaling in Rice Roots. The Plant Cell **32**, 1626-1643.

Zu P, Koch H, Schwery O, Pironon S, Phillips C, Ondo I, Farrell IW, Nes WD, Moore E, Wright GA, Farman DI, Stevenson PC. 2021. Pollen sterols are associated with phylogeny and environment but not with pollinator guilds. New Phytologist **230**, 1169-1184.

Zuo J, Niu QW, Chua NH. 2000. Technical advance: An estrogen receptor-based transactivator XVE mediates highly inducible gene expression in transgenic plants. Plant Journal **24**, 265-273.

Table 1. List of putative sterol biosynthesis inhibitors selected for analysis in Arabidopsis

Compound	Common use	Mammalian target in sterol biosynthesis	Analogous Arabidopsis enzyme(s)
Bifonazole	antifungal	CYP51A1	CYP51G1
Clotrimazole	antifungal	CYP51A1	CYP51G1
Econazole	antifungal	CYP51A1	CYP51G1
Clomiphene	SERM	EBP and DHCR24	HYD1 and DWF1
Tamoxifen	SERM	EBP and DHCR24	HYD1/DWF1
Perphenazine	antipsychotic, CaM antagonist	EBP and DHCR24	HYD1/DWF1
Fluphenazine	antipsychotic, CaM antagonist	EBP	HYD1
Acitretin	retinoid antipsoratic	DHCR24	DWF1
Doxepin	antipsychotic	DHCR24	DWF1
Trifluoperazine (TFP)	antipsychotic, CaM antagonist	DHCR24	DWF1

Figures

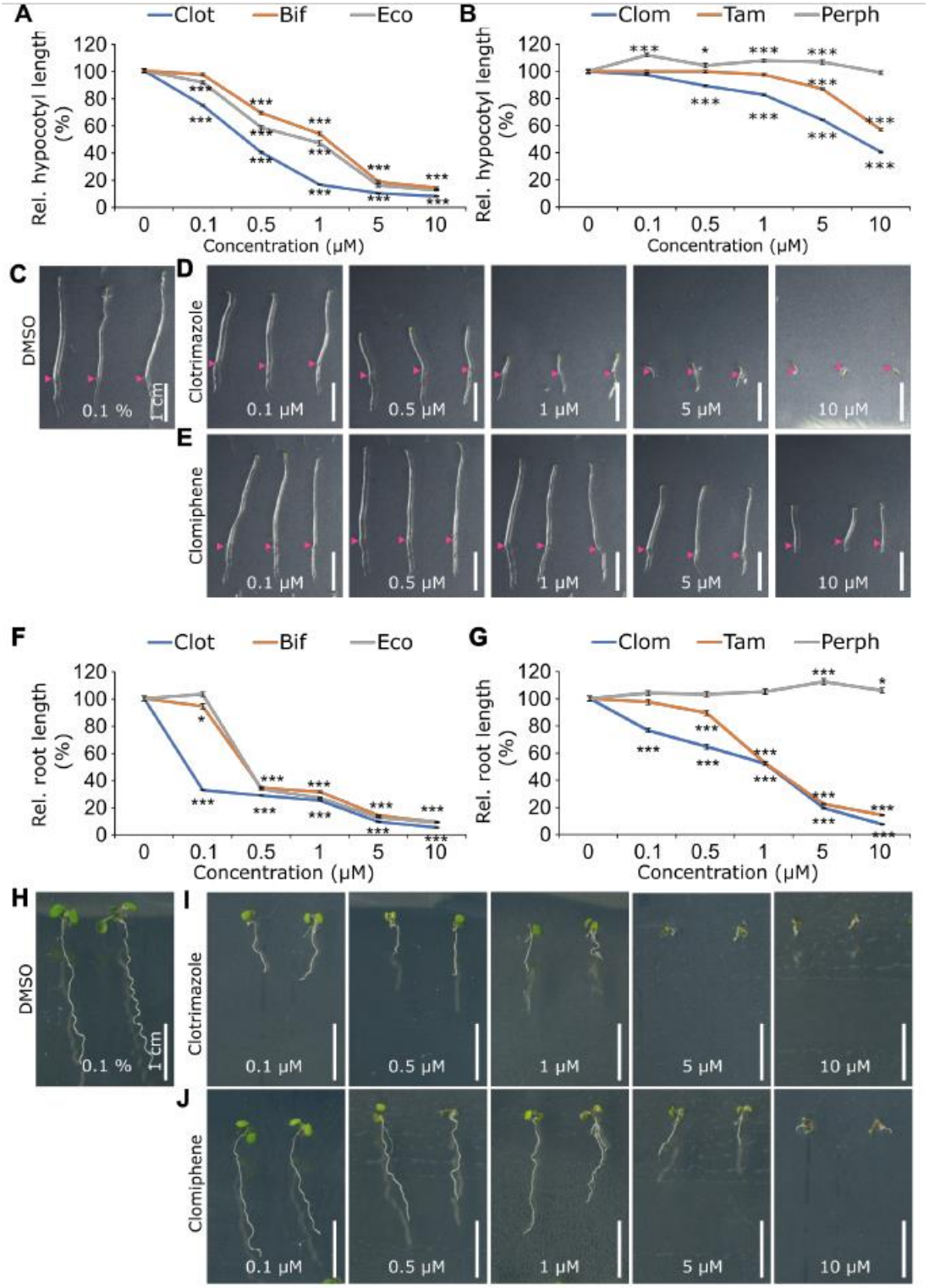
A
Clot
Bif
Eco
Rel. hypocotyl length (%)
Concentration (µM)
B
Clom
Tam
Perph
Rel. hypocotyl length (%)
Concentration (µM)
C
DMSO
0.1 %
1 cm
D
Clotrimazole
0.1 µM
0.5 µM
1 µM
5 µM
10 µM
E
Clomiphene
0.1 µM
0.5 µM
1 µM
5 µM
10 µM
F
Clot
Bif
Eco
Rel. root length (%)
Concentration (µM)
G
Clom
Tam
Perph
Rel. root length (%)
Concentration (µM)
H
DMSO
0.1 %
1 cm
I
Clotrimazole
0.1 µM
0.5 µM
1 µM
5 µM
10 µM
J
Clomiphene
0.1 µM
0.5 µM
1 µM
5 µM
10 µM

Fig. 1. Effect of putative sterol biosynthesis inhibitors on hypocotyl and root length. (A-B) Dose-response curves of hypocotyl lengths of etiolated seedlings 8 days after germination on (A) Clotrimazole (Clot), Bifonazole (Bif) or Econazole (Eco) and (B) Clomiphene (Clom), Tamoxifen (Tam) or Perphenazine (Perph). (C-E) Representative images of etiolated seedlings exposed to (C) 0.1% DMSO, (D) Clotrimazole and (E) Clomiphene. (F-G) Dose-response curves of primary root lengths of seedlings grown for 7 days under continuous illumination in presence of (F) Clotrimazole, Bifonazole or Econazole and (G) Clomiphene, Tamoxifen or Perphenazine. (H-J) Representative images of etiolated seedlings exposed to (H) 0.1% DMSO, (I) Clotrimazole and (J) Clomiphene. Averages for each condition are depicted relative to the DMSO (0.1%) control (0.1 %). n = 33 – 56 Error bars indicate ±SEM. Student's t-test p-values: *$p < 0.05$, ***$p < 0.001$. Scale bar = 1 cm.

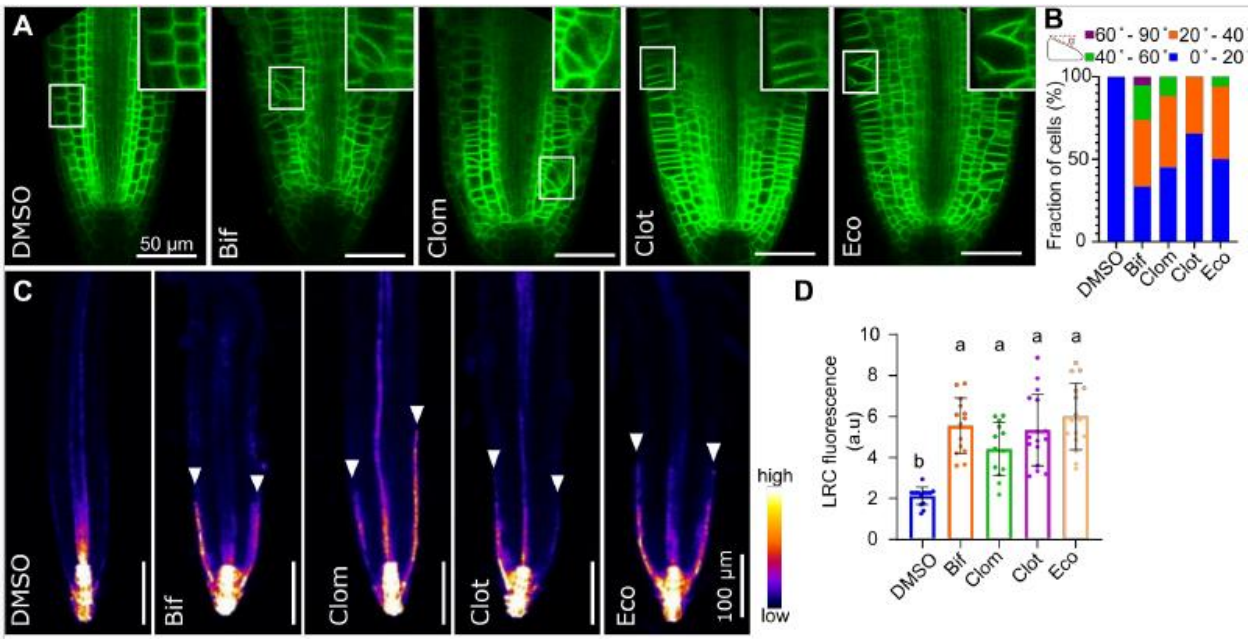

Fig. 2. Perturbed cell division orientation and auxin distribution in the root meristem after inhibitor treatment. (A) Root organization of 5 day-old ABCB19-GFP seedlings grown on media with different inhibitors Scale bar = 50 µm. (B) Quantification of anticlinal cell wall orientation of cortex cells relative to horizontal (n ≥ 5 roots, 15 cells/root). (C) Expression pattern of DR5rev::GFP in the root meristem grown on media with different inhibitors for 7 days. Scale Bar, 100 µm. Arrowheads indicate expression in the lateral root cap (LRC). Color scale indicates relative fluorescence intensities. (D) Quantification of the DR5rev::GFP signal in the LRC (n ≥ 13). Treatments are DMSO (0.1%), Bifonazole (1 µM), Clomiphene (1 µM), Clotrimazole (1 µM), Econazole (1 µM).

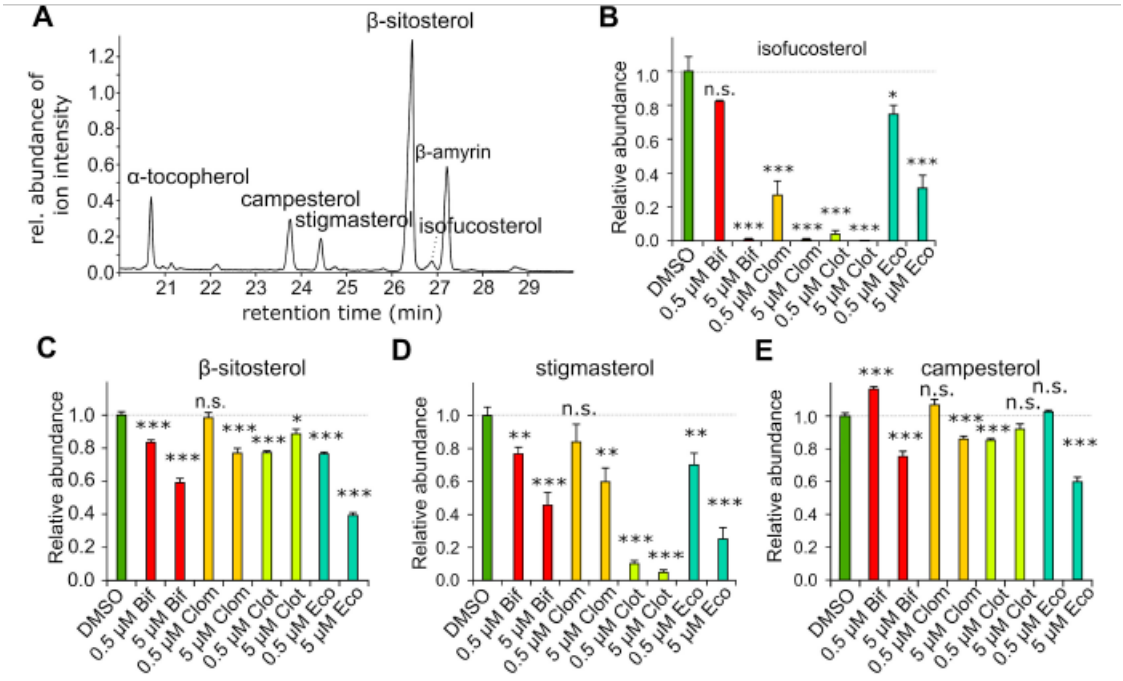

Fig. 3. Relative quantification of the major sterols after inhibitor treatment. (A) Representative Total Ion Current (TIC) GC-MS chromatogram of DMSO-treated seedlings, with annotation of the major peaks. (B-E) Peak intensities of (B) isofucosterol , (C) β-sitosterol, (D) stigmasterol and (E) campesterol in seedlings treated with two concentrations (0.5 or 5 µM) of Bifonazole (Bif), Clomiphene (Clom), Clotrimazole (Clot) and Econazole (Eco), relative to DMSO (0.1%). Error bars represent SEM. n = 5. Student's t-test *p < 0.05, **p < 0.01, ***p < 0.001. Non-significant (n.s.) p ≥ 0.05.

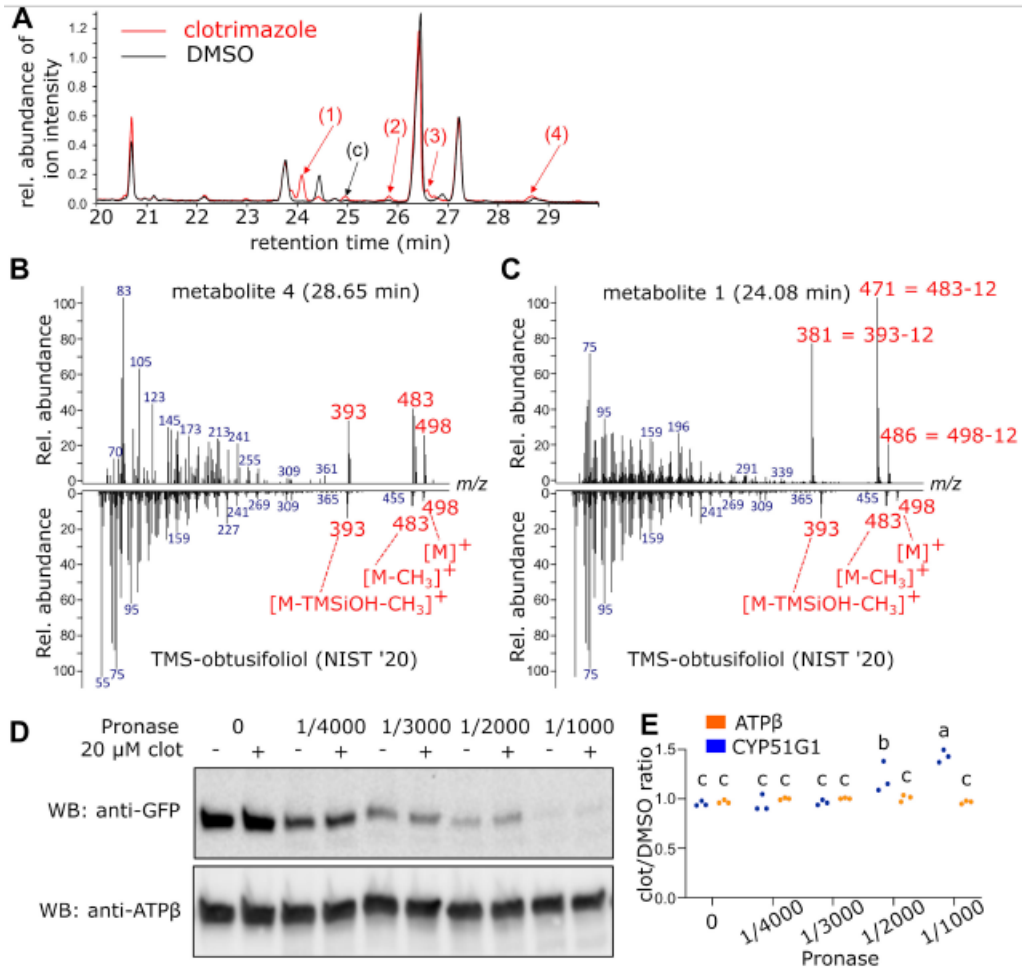

Fig. 4. Clotrimazole target identification. (A) Overlay of a representative TIC GC-MS chromatogram of a control sample and samples treated with 5 µM clotrimazole. Four new peaks induced by clotrimazole treatment are indicated by numbers. (c) is a contaminant. (B-C) Comparison of the GC-MS profile of TMS-obtusifoliol (NIST '20) to (B) metabolite 2 and (C) metabolite 1. Major fragment ions are indicated in red. (D) DARTS analysis of the protein susceptibility to proteolytic degradation. Total protein extracts of *35S::AtCYP51G1-YFP* seedlings were incubated with DMSO or clotrimazole (20 µM) and then challenged with different pronase dilutions. The AtCYP51G1-YFP protein levels were detected by protein gel blot (WB) analysis using anti-GFP and anti-ATPβ antibodies. (E) Quantification of the protein band intensity relative to the DMSO control. n=3. $p < 0.05$ by two-way ANOVA analysis followed by Tukey's multiple comparisons test. Letter code labels significant differences.

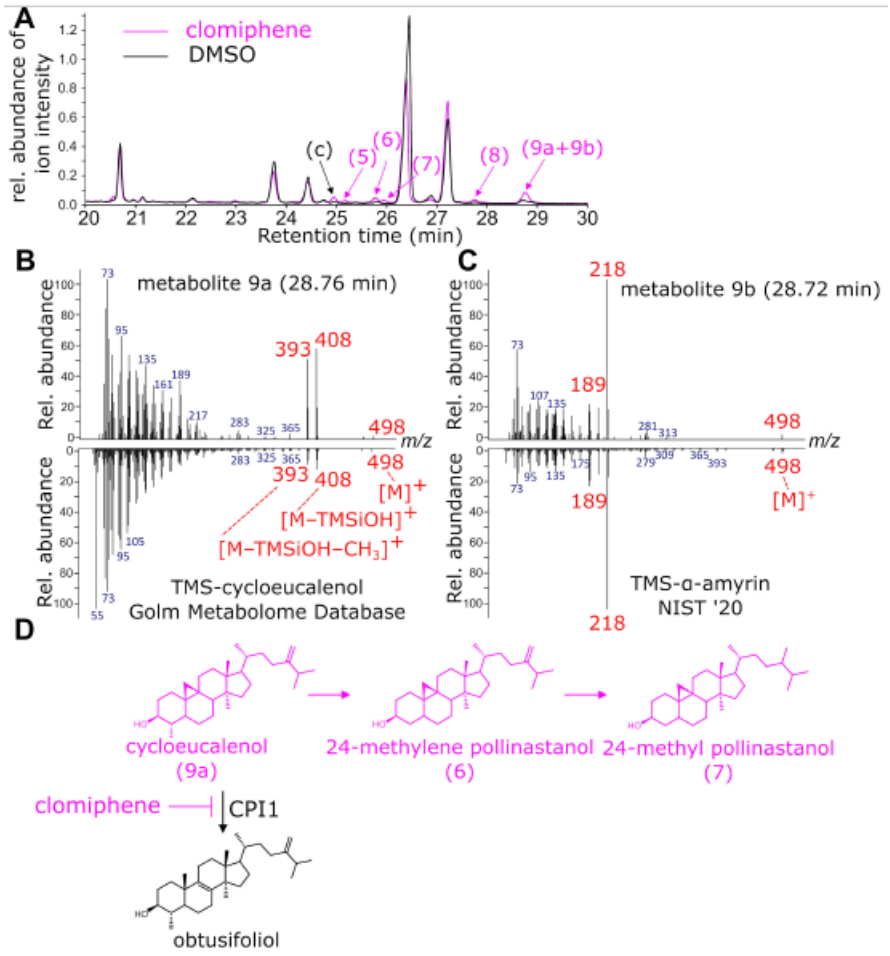

Fig. 5. GC-MS based identification of CPI1 as a clomiphene target. (A) Overlay of a representative TIC GC-MS chromatogram of the controls and the samples treated with 5 µM clomiphene. Arrows indicate the positions of the novel accumulating metabolites. (c) = contaminant. (B,C) Comparison of the GC-MS profile of Metabolite 9a to TMS-Cycloeucalenol (B) and Metabolite 9b to TMS-α-amyrin (C). Reference GC-MS profiles obtained from the Golm Metabolome Database and NIST ‘20. Major fragment ions are indicated in red. (D) Model explaining how clomiphene treatment could lead to accumulation of cycloeucalenol (metabolite 9a) and subsequent conversion to 24-methylene pollinastanol (metabolite 6) and 24-methyl pollinastanol (metabolite 7).